Proceedings Paper:
Knights, OB, Cowell, DMJ, Carpenter, TM et al. (2018) Plasmonic Gold Nanoparticles for Combined Photoacoustic Imaging and Plasmonic Photothermal Therapy Using a Pulsed Laser. In: 2018 IEEE International Ultrasonics Symposium (IUS). IUS 2018, 22-25 Oct 2018, Kobe, Japan. IEEE. ISBN: 9781538634257. ISSN: 1948-5719. EISSN: 1948-5727.

https://doi.org/10.1109/ULTSYM.2018.8579902

Plasmonic gold nanoparticles for combined photoacoustic imaging and plasmonic photothermal therapy using a pulsed laser

Oscar B. Knights*, David M. J. Cowell*, Thomas M. Carpenter*, Steven Freear*, James R. McLaughlan*†
*School of Electronic and Electrical Engineering
University of Leeds, Leeds, LS2 9JT, UK
†Leeds Institute of Cancer and Pathology
University of Leeds, Leeds, LS9 7TF, UK
J.R.McLaughlan@leeds.ac.uk

***Abstract*—Plasmonic gold nanoparticles show potential for use in a range of cancer diagnostics and therapeutics, such as photoacoustic imaging (PAI) and plasmonic photothermal therapy (PPTT). Generally in PPTT, continuous wave (CW) lasers are used to destroy cancerous tissue. However, in order to add a diagnostic component through PAI, a pulsed wave (PW) laser is needed. If PPTT can be achieved using PW lasers then combined theranostic applications with the same laser system is possible. Additionally, AuNRs can be many different sizes but exhibit equivalent surface plasmon resonances, so the size may be significant in the efficacy of these modalities. We have demonstrated the potential for gold nanorods to be used for both PAI and PPTT. The Au10s displayed the highest photoacoustic signal amplitude and PPTT efficacy. A PW laser was shown to induce significant cell death to a lung cancer cell line with a fluence below the maximum permissible exposure, indicating the possibility for cancer theranostics with a PW laser.**

***Index Terms*—gold nanoparticles, photoacoustic imaging, photothermal therapy, pulsed laser, contrast agents**

I. Introduction

Plasmonic gold nanorods (AuNRs) have shown potential for use in a range of cancer diagnostics and therapeutics, such as photoacoustic imaging (PAI) and plasmonic photothermal therapy (PPTT) due to their unique optical properties [1], [2], tuneable surface plasmon resonances (SPRs) [3], relative biocompatibility [4], and functionalisation prospects [5]. The capability to synthesise them in large quantities with highly reproducible and consistent properties is an essential trait for successful clinical translation [6]. When used as contrast agents for PAI, they can enhance the optical absorption contrast ratio between the surrounding tissues and the region of interest. To achieve a photoacoustic (PA) response from AuNRs, the stress confinement condition must be satisfied, signifying that a pulsed-wave (PW) laser must be used.

AuNRs can also be used for PPTT, whereby they act as therapeutic agents by converting the absorbed laser-light into heat and destroying the target tissue [7]. Conventionally, continuous wave (CW) lasers are used as the optical source, since this type of laser system induces hyperthermia in the target region by generating bulk heating in the tissue surrounding the AuNRs [8].

A current limitation to these techniques is that they require the use of different laser types to achieve the desired results, and combined diagnostic and therapeutic approaches are restricted. If the same laser system could be used for both PAI and PPTT then combined 'theranostic' applications would be possible, and since CW lasers cannot be used to generate a PA effect, it would require the use of a PW laser.

The combination of these two modalities could be particularly useful for application in lung cancer. An existing diagnostic technique called 'Endobronchial Ultrasound' (EBUS) is an existing diagnostic technique that enables the staging of lung cancers via needle-biopsy [9]. A bronchoscope with an ultrasound transducer located on the end is passed through the mouth and into the lung, and a channel that runs the length of the bronchoscope allows various diagnostic tools to be passed through it and provide safe access to a lung tumour from close proximity [10]. It is conceivable that if a laser fibre was incorporated into the bronchoscope, instead of the diagnostic tools, then a photoacoustic-theranostic approach may be possible by facilitating the illumination of a tumour from within the lung.

In the presented study, we consider four different sized AuNRs with similar aspect ratios and SPRs for application in both PAI and PPTT. The aim is to provide the essential groundwork for the successful translation of AuNRs from diagnostics through to therapy by focussing on the use of PW lasers for a combined theranostic approach.

II. Methods

A. Gold nanorods

Four different sized citrate-capped AuNRs with similar aspect ratios and SPRs were bought (A12, Nanopartz, USA) and their size distributions (Table I) and SPRs were confirmed via transmission electron microscopy (TEM) (Fig. 1) and spectrophotometry. These particular AuNRs were purchased due

This work was supported by the Engineering and Physical Sciences Research Council (EPSRC) grants EP/N026942/1 and EP/J021156/1.

TABLE I
DETAILS OF THE AUNRS CONSIDERED IN THIS STUDY AS MEASURED BY TEM AND SPECTROPHOTOMETRY

Name	Dimensions (w × l) [nm]	Aspect ratio	SPR [nm]
Au10	$9.9 \pm 1.1 \times 39.7 \pm 5.4$	3.98 ± 0.51	811 ± 2
Au25	$23.2 \pm 2.6 \times 85.6 \pm 9.8$	3.73 ± 0.63	803 ± 2
Au40	$39.8 \pm 4.1 \times 122.5 \pm 13.8$	3.10 ± 0.35	802 ± 2
Au50	$42.2 \pm 4.6 \times 142.0 \pm 17.0$	3.38 ± 0.41	841 ± 2

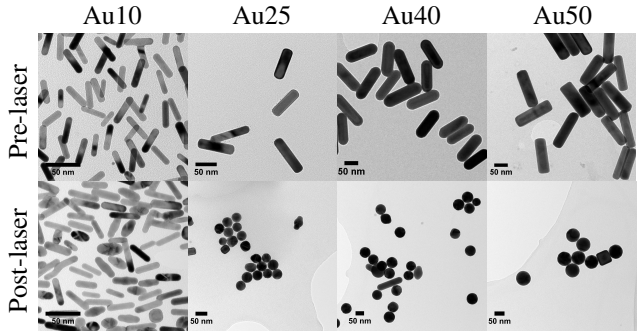

Fig. 1. Transmission electron microscope images of the Au10s, Au25s, Au40s and Au50s before (top row) and after (bottom row) pulsed laser irradiation (20 pulses, fluence $= 20\,\mathrm{mJ\,cm^{-2}}$)

to their highly reproducible properties and size distributions as 'off-the-shelf' AuNRs. The AuNRs were named according to their certified latitudinal widths: Au10 = $10\,\mathrm{nm}$, Au25 = $25\,\mathrm{nm}$, Au40 = $40\,\mathrm{nm}$, Au50 = $50\,\mathrm{nm}$.

B. Photoacoustic response

The PA response of four different sized AuNRs was measured using a pre-clinical multi-spectral optoacoustic tomographic (MSOT) system [11]. The AuNRs were made up to a concentration of $20\,\mu\mathrm{g\,ml^{-1}}$ before being sealed inside plastic straws. The straws containing AuNRs were placed into a typical turbid, agar-phantom [12] along with a straw containing water to act as a baseline. A multispectral scan was performed ($680\,\mathrm{nm}$ to $980\,\mathrm{nm}$) at six different positions to obtain an average, and the PA amplitude was calculated at the peak SPR of each sample.

The AuNRs were also imaged in a tissue-mimicking phantom using an Ultrasound Array Research Platform (UARP) II. A typical turbid agar phantom was made based on the work by Rickey et. al. [12]. A small portion of the agar mixture was combined with Au10 AuNRs at a concentration of $20\,\mu\mathrm{g\,ml^{-1}}$, set into a cylindrical shape and placed into a rectangular plastic container at a depth of $3\,\mathrm{mm}$ from the edge of the container. The rest of the agar mixture was then carefully poured into the same plastic container and left to set around the AuNR-agar inclusion.

A 128-element linear array transducer (L11-4, Verasonics Inc., WA, USA) with a central frequency $= 7.55\,\mathrm{MHz}$ and $-6\,\mathrm{dB}$ bandwidth of 90.8% was used in conjunction with the UARP II to image the phantom both actively (plane wave, 9 compounding angles) and passively (PA signal, 100 averages). A tuneable pulsed laser system (Surelite™ OPO Plus, Continuum®, USA) was used to generate the PA signal from the AuNRs (pulse width = $7\,\mathrm{ns}$, pulse repetition frequency = $10\,\mathrm{Hz}$, spot size = $5\,\mathrm{mm}$, laser fluence $= 19 \pm 2\,\mathrm{mJ\,cm^{-2}}$ at the surface of the phantom)

C. Photothermal therapy

A non-small cell lung epithelial carcinoma cell line (A549, ATCC, UK) was cultured in DMEM (Dulbecco's Modified Eagle Medium) media supplemented with $10\,\%$ FBS (Fetal Bovine Serum), and once confluent, used to seed a 96-well plate with approximately 1×10^3 cells per well. Following $24\,\mathrm{h}$ incubation, the media in all the wells were either replenished with fresh media or replaced with a media-AuNR solution at a AuNR concentration of $20\,\mu\mathrm{g\,ml^{-1}}$. The 96-well plate was then incubated for a further $24\,\mathrm{h}$, to facilitate the uptake of AuNRs by the lung cancer cells, before being exposed to laser irradiation.

For comparison, two laser systems were used to perform PPTT on the A549 cells. A CW diode laser (B4, Sheaumann) operating at $0.5\,\mathrm{W}$ (spot size $= 8\,\mathrm{mm}$) and a tuneable pulsed laser system (the same used in the PA study) with a laser pulse fluence of $25 \pm 1\,\mathrm{mJ\,cm^{-2}}$. Both of the laser fibres were mounted to a 3-axis motorised stage and scanned across the 96-well plate. Each well was irradiated for $5\,\mathrm{min}$ from above the plate, while an infrared (IR) thermal imaging camera (thermoIMAGER TIM 640, Micro-epsilon-Messtechnik GmbH & Co KG, Germany) recorded a frame every second for the duration of the exposure. Due to the limitations of IR cameras, the measurements represent the temperature of the bottom of the plastic 96-well plate.

This method was repeated for a 96-well plate that contained only cells (no AuNRs) as well as several plates where the AuNR-media solution in each well was replaced with fresh media immediately before laser irradiation to reduce any free-floating AuNRs.

III. RESULTS AND DISCUSSION

The results from the MSOT system (Fig. 2a) show that the smallest of the AuNRs (Au10s) produced the strongest PA signal, with an amplitude of more than three times that of the Au25s and Au40s. This suggests that, at equivalent total mass across different sized AuNRs, smaller AuNRs ($< 25\,\mathrm{nm}$) are the most effective PA-converters. Since the Au10s produced the strongest PA signals, a tissue-mimicking phantom was made with an inclusion of Au10s at a concentration of $20\,\mu\mathrm{g\,ml^{-1}}$. Fig. 2b shows the reconstructed B-mode image of the phantom with the PA image of the inclusion overlaid. The bright spot seen at a depth of approximately $17\,\mathrm{mm}$ is a result of the high-intensity laser pulse hitting the back of the phantom (as the laser was at a slight angle to accommodate the ultrasound probe) and generating a strong PA signal. However, at increased depths the AuNR inclusion is visible. At a depth of $3 - 8\,\mathrm{mm}$, the phantom containing Au10s approximately mimics typical depths relating to endobronchial ultrasound

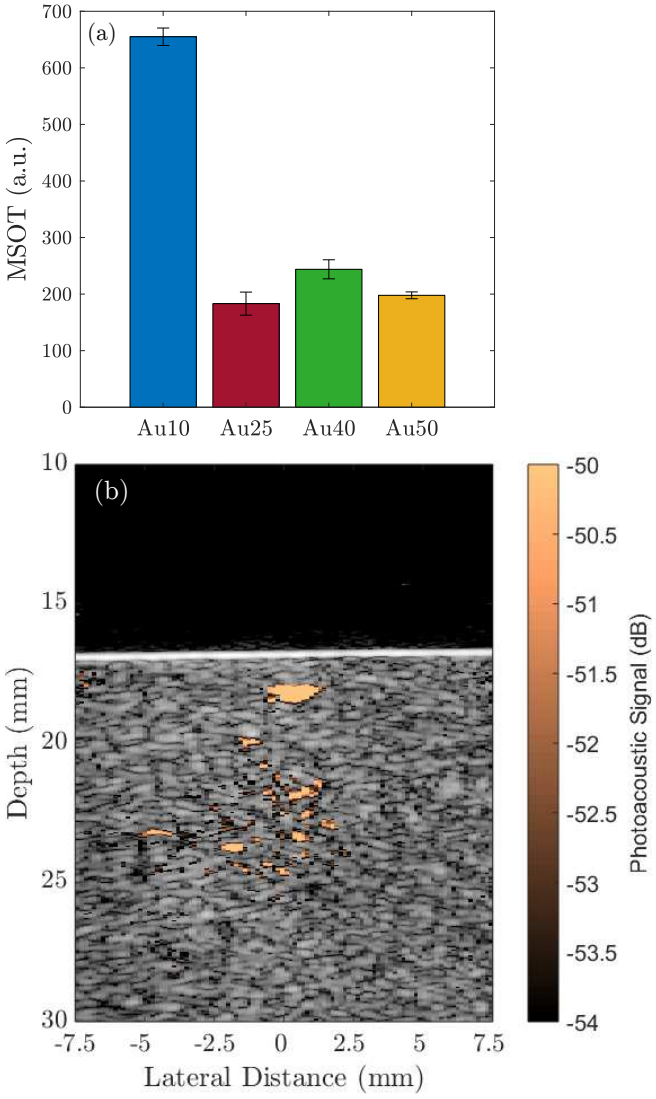

Fig. 2. (a) The photoacoustic amplitude of four different sized AuNRs with certified lateral widths of 10 nm (Au10), 25 nm (Au25), 40 nm (Au40), and 50 nm (Au50), measured with a MSOT system. (b) A B-mode plane-wave image (9 compounding angles) of a tissue-mimicking agar phantom with an overlaid photoacoustic image generated by a 5 mm diameter inclusion of Au10 AuNRs (concentration $20\,\mu g\,ml^{-1}$) at a depth of 3 mm below the surface and a laser fluence $= 15 \pm 2\,mJ\,cm^{-2}$ at the surface. The PA signal is referenced to the maximum of the B-mode image (dB).

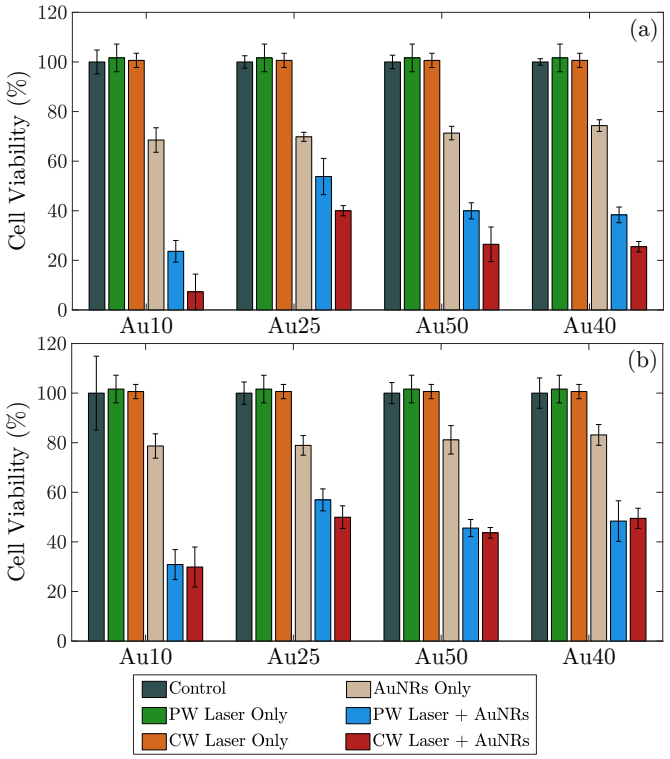

Fig. 3. Lung cancer cell viability (A549) after PW laser exposure only (green), CW laser exposure only (orange), incubation with AuNRs without laser exposure (beige), incubation with AuNRs combined with PW laser exposure (blue), and incubation with AuNRs combined with CW laser exposure (red). (a) AuNR-media was not replaced before laser irradiation (i.e. free-floating AuNRs remained), and (b) free-floating AuNRs were removed before laser irradiation by replacing the AuNR-media solution with fresh media. AuNR concentration $= 20\,\mu g\,ml^{-1}$, PW laser fluence $= 25 \pm 1\,mJ\,cm^{-2}$ and CW power $= 0.5$ W for all data points.

of lung tumours. The non-uniform signal from the Au10s is likely due to an inhomogeneous distribution of AuNRs throughout the inclusion, as a direct result of making the inclusion. The results demonstrate the ability for AuNRs to be used as contrast agents for PAI of lung tumours.

The PPTT efficacy of the four different AuNR sizes was determined under both PW and CW laser irradiation. The PW laser fluence was $25 \pm 1\,mJ\,cm^{-2}$ (below $31\,mJ\,cm^{-2}$, the maximum permissible exposure of laser irradiation to skin [13]) and the CW power output was 0.5 W. Fig. 3a shows the cell viability of the A549 cells under various parameters and with the free-floating AuNRs remaining. When the cells were illuminated by the PW or CW laser only, without incubation with AuNRs, no cell death was observed. However, once the different sized AuNRs were incubated with the cells for 24 h to facilitate uptake of the AuNRs by the cells, significant cell death was observed for all AuNR sizes under both PW and CW laser irradiation. The data indicate the importance of both AuNRs and laser irradiation to induce cell death. The CW laser showed the highest cell toxicity across all four AuNR sizes compared with the PW laser, however this was likely due to the bulk heating effect observed as a result of the free-floating AuNRs remaining in each of the wells. Fig. 4a shows a single frame taken with the IR camera displaying the temperature difference between the well under PW (green circle) and CW (blue circle) laser irradiation. Fig. 4b & 4c show an example of the temperature profile of the cells under CW and PW laser irradiation, and the temperature of the wells under CW exposure can be seen to have increased several degrees.

The PPTT study was repeated with the free-floating AuNRs removed from each well by replacing the AuNR-media solution with fresh media, leaving the AuNRs that were either internalised by the cells or stuck to the surface of the cells (Fig. 3b). Significant cell death ($< 60\%$) was also observed

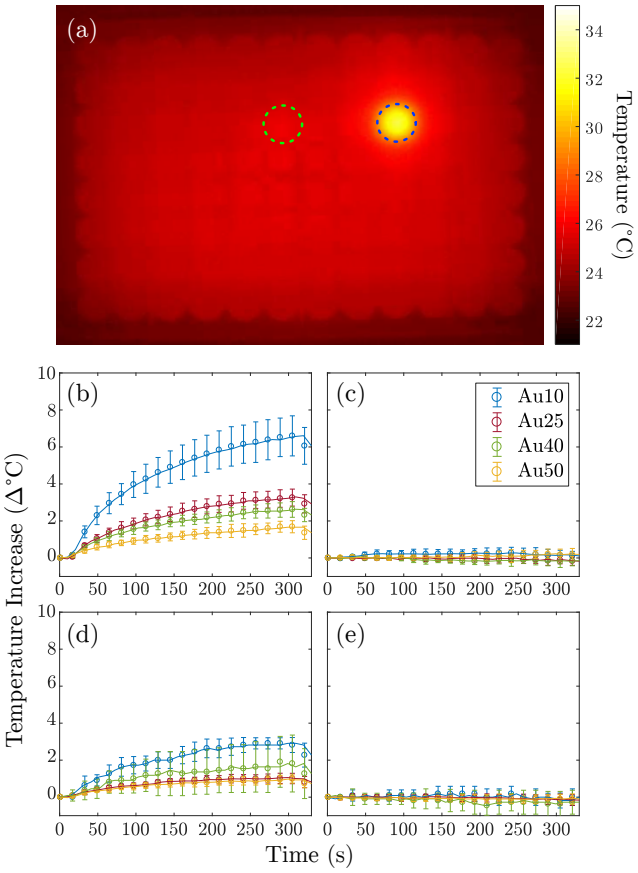

Fig. 4. (a) Infrared thermal image of the bottom of a 96-well plate containing A549 cells and Au40 AuNRs during laser irradiation with both a PW (green circle) and CW (blue circle) laser, and the temperature profile of the cells under (b) CW laser irradiation with free-floating AuNRs, (c) PW laser irradiation with free-floating AuNRs, (d) CW laser irradiation with free-floating AuNRs removed and (e) PW laser irradiation with free-floating AuNRs removed. Due to the limitations of infrared cameras, the measured temperature is that of the bottom of the 96-well plate.

for the cells incubated with all AuNR sizes and exposed to laser irradiation. However, the cellular toxicity induced by both the PW and CW lasers was comparable in this case, indicating that the removal of free-floating AuNRs reduced the PPTT efficacy of the CW laser. Fig. 4d & 4e show an example of the temperature profile of the cells under CW and PW laser irradiation, and the temperature of the wells under CW displayed a reduced temperature increase compared with that of the free-floating AuNRs. The data suggest that PW are able to perform PPTT of lung cancer at fluence levels below the safe exposure limit.

The photostability of the four different AuNRs was measured after 20 laser pulses with a fluence of $20\,\mathrm{mJ\,cm^{-2}}$. Fig. 1 shows TEM images of each AuNR size before (top row) and after laser irradiation. The images clearly show that almost the entire population of Au25s, Au40s and Au50s had melted into complete spheres, whereas the Au10s appeared to resist complete melting and still retain a significant portion of rod-shaped particles. This indicates the increased photostability of the Au10s and potentially smaller AuNRs in general.

IV. Conclusions

We have shown that AuNRs have the potential to be used for both diagnostic and therapeutic modalities such as PAI and PPTT. The use of PW lasers for PAI is evident, and we have demonstrated that PPTT is also possible with a PW laser at laser fluence levels below the MPE for skin. Significant cell death was observed for all AuNR sizes when combined with both PW and CW laser irradiation, however laser irradiation alone was not sufficient. The AuNR sizes had an effect on overall PPTT efficacy and the smallest AuNRs (Au10s) induced the highest cell-death.

Acknowledgment

Oscar B. Knights would like to acknowledge the EPSRC for supporting his PhD through the Doctoral Training Grant Studentship. James R. McLaughlan would like to acknowledge support from an EPSRC Innovation Fellowship (EP/S001069/1) and the Royal Society (RG170324).

References

[1] S. Eustis and M. A. El-Sayed, "Why gold nanoparticles are more precious than pretty gold: Noble metal surface plasmon resonance and its enhancement of the radiative and nonradiative properties of nanocrystals of different shapes," *Chem. Soc. Rev.*, vol. 35, pp. 209–217, 2006.

[2] Y. Huang, K. Xia, N. He, Z. Lu, L. Zhang, Y. Deng, and L. Nie, "Size-tunable synthesis of gold nanorods using pyrogallol as a reducing agent," *Science China Chemistry*, vol. 58, no. 11, pp. 1759–1765, 2015.

[3] A. Bouhelier, R. Bachelot, G. Lerondel, S. Kostcheev, P. Royer, and G. P. Wiederrecht, "Surface plasmon characteristics of tunable photoluminescence in single gold nanorods," *Phys. Rev. Lett.*, vol. 95, p. 267405, Dec 2005.

[4] A. M. Alkilany and C. J. Murphy, "Toxicity and cellular uptake of gold nanoparticles: what we have learned so far?" *Journal of Nanoparticle Research*, vol. 12, no. 7, pp. 2313–2333, 2010.

[5] A. M. Alkilany, L. B. Thompson, S. P. Boulos, P. N. Sisco, and C. J. Murphy, "Gold nanorods: their potential for photothermal therapeutics and drug delivery, tempered by the complexity of their biological interactions," *Advanced drug delivery reviews*, vol. 64, no. 2, pp. 190–199, 2012.

[6] S. Jain, D. G. Hirst, and J. M. O'Sullivan, "Gold nanoparticles as novel agents for cancer therapy," *The British Journal of Radiology*, vol. 85, no. 1010, pp. 101–113, Feb. 2012.

[7] X. Huang and M. A. El-Sayed, "Plasmonic photo-thermal therapy (pptt)," *Alexandria Journal of Medicine*, vol. 47, no. 1, pp. 1–9, 2011.

[8] W. I. Choi, A. Sahu, Y. H. Kim, and G. Tae, "Photothermal cancer therapy and imaging based on gold nanorods," *Annals of biomedical engineering*, vol. 40, no. 2, pp. 534–546, 2012.

[9] K. Yasufuku, M. Chiyo, E. Koh, Y. Moriya, A. Iyoda, Y. Sekine, K. Shibuya, T. Iizasa, and T. Fujisawa, "Endobronchial ultrasound guided transbronchial needle aspiration for staging of lung cancer," *Lung cancer*, vol. 50, no. 3, pp. 347–354, 2005.

[10] M. Gomez and G. A. Silvestri, "Endobronchial ultrasound for the diagnosis and staging of lung cancer," *Proceedings of the American Thoracic Society*, vol. 6, no. 2, pp. 180–186, 2009.

[11] V. Ntziachristos and D. Razansky, "Molecular imaging by means of multispectral optoacoustic tomography (msot)," *Chemical reviews*, vol. 110, no. 5, pp. 2783–2794, 2010.

[12] D. W. Rickey, P. Picot, D. Christopher, and A. Fenster, "A wall-less vessel phantom for doppler ultrasound studies," *Ultrasound in medicine & biology*, vol. 21, no. 9, pp. 1163–1176, 1995.

[13] American National Standard for Safe Use of Lasers, *ANSI*, Std., 2014.